

tural location and by their characteristic combinations of somatic sensory and motor inputs. All three nuclei project in a spatially overlapping manner to parietal cortex and terminate in the cortical layers as summarized in Fig. 2. This arrangement of somatic sensory and motor thalamocortical fiber systems in the marsupial opossum stands in contrast to that reported for placental mammals with the use of comparable techniques; for example, in the cat, the ventral posterior nucleus projects to layers IV and III of postcruciate cortex, while VL projects only to precruciate cortex (6). These anatomical species differences were predicted by parallel differences in physiological mapping results in the opossum and cat (3, 7). In the opossum, the convergent projections from separate sensory and motor thalamic nuclei onto a single cortical area comprise an adequate anatomical correlate for a functionally amalgamated sensory-motor area.

The identification of three separate thalamic inputs to sensory cortex is not unique to the somatic sensory system of the opossum, since more than one input has already been reported for opossum visual cortex and hedgehog visual, auditory, and somatic sensory cortices (8). In sensory systems of both species, the results demonstrate that more than one thalamic influence is operating directly on each "column" of sensory cortex. Multiple thalamic inputs that terminate in different combinations of cortical layers provide a probable anatomical substrate for the variety of responses evoked in cortex after stimulation of different thalamic nuclei. For example, the restricted VP projection provides a reasonable substrate for the primary evoked response while the diffuse CIN projection may well underlie the recruiting response first discovered by Morison and Dempsey (1). However, further studies which combine anatomical and physiological techniques are necessary in order to more closely correlate physiological responses with their anatomical substrate.

H. KILLACKEY  
F. EBNER

Section of Neurosciences, Division of  
Biological and Medical Sciences,  
Brown University, Providence,  
Rhode Island 02912

#### References and Notes

1. R. Morison and E. O. Dempsey, *Amer. J. Physiol.* **135**, 281 (1942).
2. O. Creutzfeldt, H. Lux, S. Watanabe, in *The Thalamus*, D. Purpura and M. Yahr, Eds.

- (Columbia Univ. Press, New York, 1966); C. L. Li, C. Cullen, H. Jasper, *J. Neurophysiol.* **19**, 111, 131 (1956).
3. R. Lende, *Science* **141**, 730 (1963).
  4. T. Walsh and F. Ebner, *J. Comp. Neurol.*, in press.
  5. R. Fink and L. Heimer, *Brain Res.* **4**, 369 (1967).
  6. P. Hand and A. Morrison, *Exp. Neurol.* **26**, 291 (1970); E. Jones and T. Powell, *Brain Res.* **13**, 298 (1969); P. Strick, *ibid.* **20**, 130 (1970).
  7. C. Woolsey, in *Biological and Biochemical Basis of Behavior*, H. Harlow and C. Woolsey,

Eds. (Univ. of Wisconsin Press, Madison, 1958).

8. L. Benevento and F. Ebner, *J. Comp. Neurol.* **143**, 242 (1971); W. Hall, *Anat. Rec.* **166**, 313 (1970); H. Killackey, *ibid.* **172**, 345 (1972); — and F. Ebner, *Brain Behav. Evol.*, in press; R. Ravizza and I. T. Diamond, *Anat. Rec.* **172**, 390 (1972).
9. T. Walsh and R. Ebner, *J. Anat.* **107**, 1 (1970).
10. Supported by NINDS grant NS-06551 and fellowship NS-50714 (to H.P.K.). We thank E. W. Swick and E. DiPalma for assistance.

15 June 1972

## Three-Dimensional Structure of Yeast Phenylalanine Transfer RNA: Folding of the Polynucleotide Chain

**Abstract.** At 4 Å resolution the polynucleotides in yeast phenylalanine transfer RNA are seen in a series of electron dense masses about 5.8 Å apart. These peaks are probably associated with the phosphate groups, while lower levels of electron density between segments of adjacent polynucleotide chains are interpreted as arising from hydrogen-bonded purine-pyrimidine base pairs. It is possible to trace the entire polynucleotide chain with only two minor regions of ambiguity. The polynucleotide chain has a secondary structure consistent with the cloverleaf conformation; however, its folding is different from that proposed in any model. The molecule is made of two double-stranded helical regions oriented at right angles to each other in the shape of an L. One end of the L has the CCA acceptor; the anticodon loop is at the other end, and the dihydrouridine and TΨC loops form the corner.

Transfer RNA (tRNA) has a key role in the translation of the polynucleotide sequences of messenger RNA into the polypeptide sequences of protein. A considerable body of information has accumulated regarding these molecules but up to the present time the three-dimensional folding of the polynucleotide chain was unknown. Eight years ago Holley and his collaborators sequenced alanine tRNA from yeast and pointed out that the sequence could be folded into a cloverleaf conformation in which there are four base paired stem regions connected with loops (1). Approximately 40 tRNA molecules from various sources have now been sequenced, and all of them can be arranged in a similar cloverleaf arrangement. We have been carrying out an x-ray diffraction analysis of yeast phenylalanine tRNA (2) whose sequence is known (3). Recently we described the heavy atom derivatives which allowed us to calculate a three-dimensional electron density map at 5.5 Å resolution (4). That map allowed us to discern the external shape of portions of the molecule and to trace short segments of the polynucleotide chain. We have continued this work and now report our interpretation of the electron density map at 4.0 Å resolution which allows us to determine the positions of most of the phosphate groups in the nucleotides of yeast phenylalanine tRNA. The polynucleo-

tide chain has been traced and its three-dimensional folding is presented.

Yeast phenylalanine tRNA crystallizes in an orthorhombic unit cell, space group  $P_{21}22_1$ ,  $a = 33$  Å,  $b = 56$  Å, and  $c = 161$  Å, with four molecules in the unit cell (2). The methods used in preparing crystals of yeast phenylalanine tRNA, and the chemistry of the isomorphous heavy atom replacements have been described (4). Three types of heavy atom derivatives containing platinum, osmium, or samarium have been used. The 4 Å data including anomalous pairs were collected for the osmium and samarium derivatives and 5.5 Å data were collected for the platinum derivative. The positions of these heavy atoms have been reported (4). The overall figure of merit for the 2806 reflections collected is 0.70, and the R factors (modulus) are 0.58 for osmium 5.5 Å data; 1.56 for the 5.5 Å to 4.0 Å data; 0.47 for the 4.0 Å samarium data; and 1.05 for the 5.5 Å platinum data (4).

The electron density map reported at 5.5 Å resolution (4) had a number of intense peaks 5 to 7 Å apart, which were interpreted as arising from the phosphate groups of the tRNA polynucleotide chain. Although portions of the polynucleotide chain could be traced at 5.5 Å resolution, there were too many ambiguities to trace the entire chain. However, at 4.0 Å resolution the individual peaks of electron

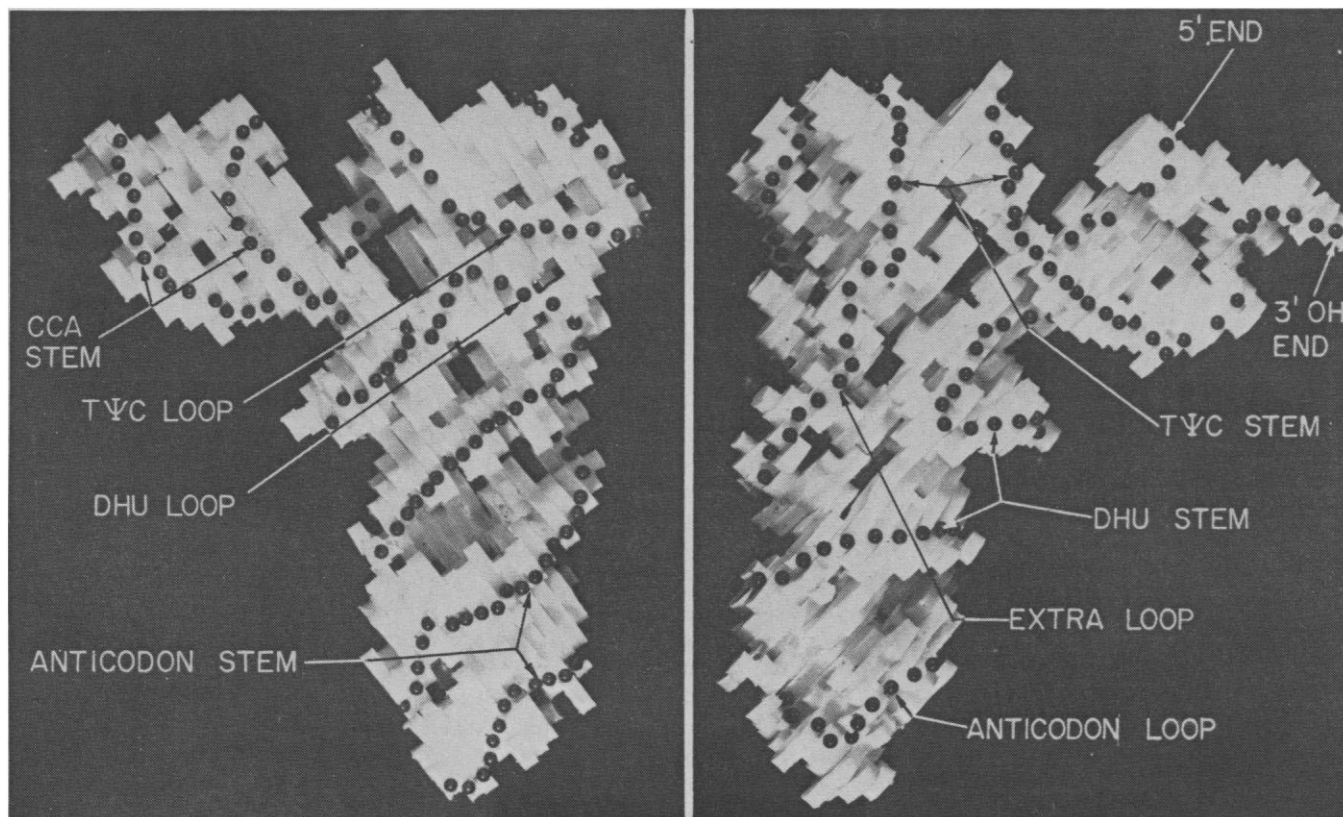


Fig. 1. Two views from opposite sides of a solid molecular model of yeast phenylalanine tRNA as seen at 4.0 Å resolution. The molecule is approximately 20 Å thick in a direction perpendicular to the page. The vertical distance in the molecule is 77 Å. In order to make the tracing of the chains more visible, a series of round-headed pins have been inserted into the molecule. These do *not* represent atoms, but are designed to show the folding of the polynucleotide chain. Hydrogen-bonded base paired stem regions can be readily identified because the adjacent polynucleotide chains are connected to each other.

density are largely resolved. We can observe approximately 80 substantial peaks of electron density in the asymmetric unit. Since yeast phenylalanine tRNA contains 76 nucleotides as well as a number of tightly bound cations, this number was considered adequate for the interpretation of the map.

As was pointed out in the 5.5 Å analysis, large portions of the tRNA molecule can be visualized directly because the tRNA molecules are clearly separated from neighboring molecules by large regions of mother liquor. This includes the unusual 20 to 30 Å separations between the molecules along the *c* axis (4). However, portions of the molecule along the *a* and *b* axes are closely packed next to neighboring molecules. The shape of the molecule as described at 5.5 Å resolution was largely correct, except for one region of electron density which appeared to be attached at the end of the elongated molecule. In the 4 Å map, it is apparent that this region is attached to the side of an adjacent molecule and thus the molecule is L-shaped. A solid three-dimensional model of the molecule has been made at 4.0 Å resolution, and two views are shown in Fig. 1. The

sequence of yeast phenylalanine tRNA is shown in Fig. 2.

The peaks of electron density in the map occur with an average separation of 5.8 Å. This spacing is close to that expected from adjacent phosphate groups on a polynucleotide chain. However, individual spacings vary. This would be anticipated in a molecule that had not only a regular polynucleotide conformation in helical regions but also less regular conformations that occur in other parts of the molecule. Interpretation of the electron density map was aided considerably by the observation that there are four regions in the map in which two adjacent chains of electron dense peaks are connected through regions of lowered electron density. The lower electron density regions typically connect two chains as shown in the electron density maps in Fig. 3. In Fig. 3a there are two polynucleotide chains perpendicular to the page, and the phosphate peaks are designated by *X*. It can be seen that the two high density chains are connected by a lower density region which lies largely on one side of both chains. Because of the asymmetry in the geometry of polynucleotide

chains, this suggests that we are observing pairs of hydrogen-bonded bases connecting the two chains, each of which has opposite polarity and is running in opposite directions.

Another region connecting two polynucleotide chains is shown in Fig. 3b. Here we can see the trace of two polynucleotide chains rising toward the reader and then dipping down. Peaks representing the phosphate groups on the polynucleotide chain are marked, and there is a region of weaker electron density connecting the two chains. Four such regions are found in the map and are interpreted to be right-handed, anti-parallel double-stranded stems.

The 3'-OH terminus of the molecule is single-stranded and has the only ribose which contains free *cis*-OH groups. Careful inspection of the electron density map revealed that a segment of extended chain containing four peaks of electron density went from one molecule to an adjoining molecule approximately 22 Å away. Since there was no other polynucleotide chain nearby, it seemed to be a suitable candidate for the CCA end (5). In addition, the terminal phosphate peak was 7.0 Å away from the heavy atom osmium po-

sition. Osmium forms complexes with ribonucleotides through the 2'- and 3'-OH groups, and it seems likely that the osmium is complexed in tRNA to the terminal adenosine. Through a study of related osmium complexes we estimate the distance between osmium and the next phosphate group on the chain could be between 4.0 and 7.6 Å, depending on the orientation of the phosphate. The observed position of the osmium atom next to the phosphate group at the end of this single chain of four residues led us to infer that this was the 3'-OH end of the molecule.

Initial attempts at tracing the polynucleotide chain involved a simple inspection of the electron density map to determine which peaks were within a reasonable distance to be considered as adjoining phosphates on a polynucleotide chain. When a polynucleotide chain is fully extended, it has a phosphate-to-phosphate distance of approximately 7.5 Å; however, the chain can be folded so that in some cases the distance between the phosphates can be less than 5 Å. Accordingly, we carried out the chain tracing by looking for the nearest neighbors within that distance range. Study of the three-dimensional electron density map revealed that only a small number of chain tracings were possible. In most regions the chain can be traced unambiguously; however, in a few places in the map the electron density of a peak was somewhat decreased so that we could not be certain that it was a nucleotide phosphate group. Alternatively, in two places too many peaks were clustered together, so that it was not easy to make an unambiguous assignment of correct neighbors. However, it quickly became apparent that one of the chain tracings not only provided a reasonable assignment of nearest neighbor relations but also demonstrated a direct and simple physical arrangement which embodied the secondary structure implicit in the cloverleaf model. The four double helical regions described above only occurred along portions of the chain in which base pairing is expected in the cloverleaf conformation. This correlation between the hydrogen-bonded base pairs in the cloverleaf and the low electron density regions between chains in the map gave us more confidence that this was the correct chain tracing. In this regard it should be pointed out that the evidence for the existence of the base pairing in the cloverleaf stems is based not only on the sequence of a large number of tRNA molecules but also on recent high-resolution nuclear

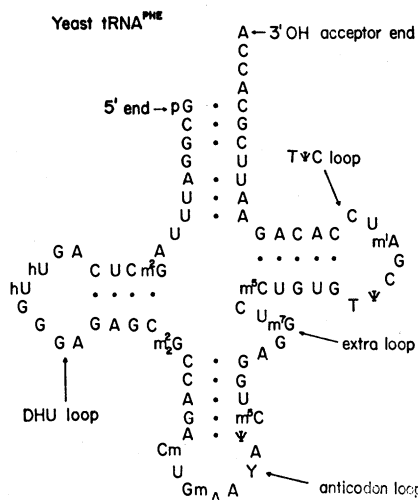
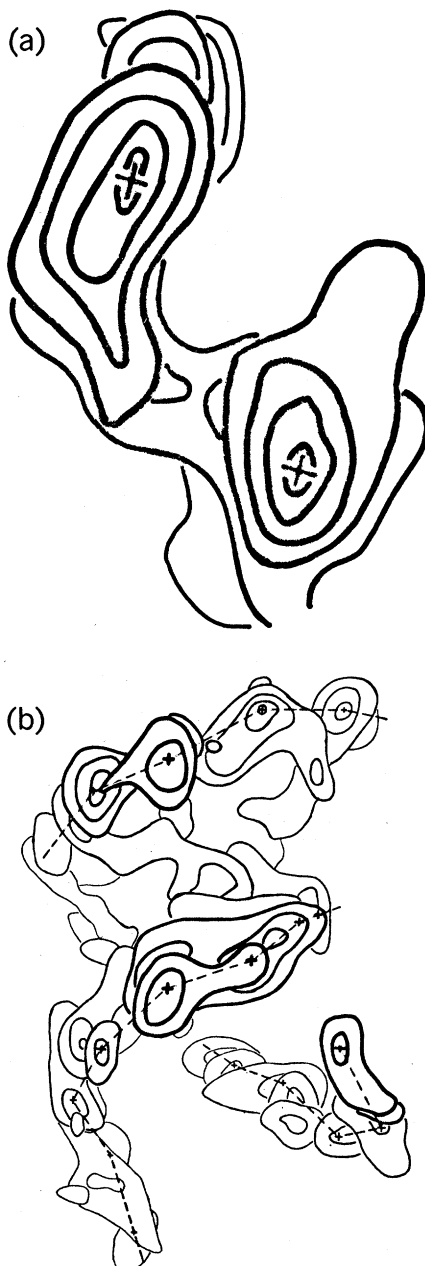


Fig. 2. The sequence of nucleotides in yeast phenylalanine tRNA shown in the conventional cloverleaf diagram (3).



magnetic resonance studies of yeast phenylalanine tRNA in solution (6). Accordingly, the chain tracing found in the three-dimensional electron density map which appeared to utilize the base pairing in the stems of the cloverleaf was selected as the correct tracing. However, it should be noted that one or two alternative tracings are still considered possible at 4.0 Å resolution if one ignores the evidence for the cloverleaf secondary structure. At the present time we are collecting 3 Å data, and it is anticipated that it will allow us to remove any remaining uncertainties regarding the course of the polynucleotide chain.

The folding of the molecule is illustrated in the photographs of the solid model shown in Fig. 1 as well as in the perspective drawing of Fig. 4. The molecule contains two segments of double helix, each about one turn in length. These are oriented at approximately right angles to each other to form an L. The CCA stem is connected to the TΨC stem in a continuous double helix in which the two helical axes of the stem regions are nearly colinear. The TΨC loop occurs at the corner of the L-shaped molecule. Immediately adjoining it is the DHU loop, whose stem is connected to the CCA stem through a short segment of chain containing two phosphate groups. Both the DHU stem and the anticodon stem form the other continuous double helix around an axis that is oriented approximately at right angles to the axis containing the CCA and TΨC stems. The anticodon loop is located at the very end of the molecule while the DHU loop is in a position immediately adjoining the TΨC loop at the corner of the molecule. The arrangement of these chains is shown diagrammatically in Fig. 5.

Fig. 3. Sections of the electron density map which illustrates the connections between adjacent segments of polynucleotide chain. (a) Two polynucleotide chains are shown at several levels of the electron density map. The ribose phosphate chains run perpendicular to the page. X marks the position of the phosphate peaks, and lower levels of electron density are seen to connect these chains (scale 1 cm = 2.5 Å). (b) A superposition of segments of the electron density map showing portions of three polynucleotide chains. The two chains on the left are joined by regions of lower electron density. The chain on the lower right, although passing nearby, is not joined. X marks the position of the phosphate peaks, and the dotted line shows the continuity of the ribose phosphate polynucleotide chain (scale, 1 cm = 4.7 Å).

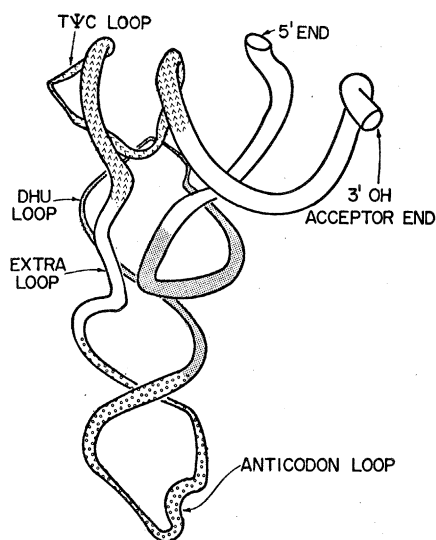


Fig. 4. A perspective diagram in which the polynucleotide chain is represented as a continuous coiled tube. The different shading represents the various loops and stem regions of the tRNA molecule. It can be seen that the TΨC and DHU loops come in very close contact.

The major part of the molecule containing the anticodon loop at one end and the TΨC loop at the other end is 77 Å long. The distance from the anticodon to the end of the CCA stem is 82 Å. An unusual feature of the molecule that was not immediately apparent is the fact that almost the entire structure appears to be 20 Å thick, which is the thickness of an RNA double helix.

It is interesting to note that the major framework of the molecule is due to two segments of helical RNA, each of which is approximately one turn in length. These two helical segments are joined by additional nucleotides in two places. A shorter stretch involves the nucleotides in positions 8 and 9, which connect the CCA stem with the DHU stem. The longer stretch contains five nucleotides in the extra loop and connects the TΨC stem with the anticodon stem. In this regard it is interesting that the extra loops in other tRNA molecules have lengths ranging from 4 to 21 nucleotides (7). We estimate that it would be possible to connect the two helical segments by using as few as four nucleotides, and it is clear from the position of the extra loop on the outside of the molecule that there is ample room there to accommodate a much larger number of nucleotides, even a group containing another elongated stem region, such as is found in some tRNA's with longer extra loop regions.

A number of attempts have been made to predict the three-dimensional

structure of tRNA by constructing models (7). Almost all of the proposed molecular models contain some of the features which are found in three-dimensional structure of tRNA. This is related to the fact that all of them use the secondary structure of the cloverleaf as the basis for their models; however, none of them describe the structure as we now see it. In several models (7) the stems of the various arms are joined to make a continuous double helix, in some cases involving a coaxial arrangement of the CCA stem and the TΨC stem as well as the DHU and anticodon stems; however, none of them illustrate the arrangement of these two helical regions at right angles to each other as is observed in the electron density map.

It is worth drawing attention to some features in the molecule. It has been reported that photoactivation of *Escherichia coli* tRNA<sup>Val</sup><sub>1</sub> results in the formation of a photodimer involving the 4-thioU residue found in position 8 and the cytosine in position 13 (8). This suggests that these two bases are in close proximity, and this feature has been incorporated in some models. In the electron density map the distance between the phosphates of residues 8 and 13 is near 10 Å, a distance close enough to allow the formation of a photodimer. In all tRNA's so far sequenced the base at position 15 was found to be complementary to the base between the TΨC stem and the extra arm (base 48 in yeast phenylalanine tRNA) (9). The phosphates of these residues are 16 Å apart in our present map, a distance which is compatible with the existence of a base pair. However, the visualization of the purine and pyrimidine bases is necessarily crude at 4 Å resolution, and we will await the analysis of the 3 Å map before citing in detail which interactions stabilize the three-dimensional conformation of tRNA.

A number of enzymatic cleavages, base specific chemical modifications, and oligonucleotide binding studies on native tRNA have been described (7), and most of these seem compatible with the structure we see in the map. A thorough discussion of these reactions together with a discussion of the possible mechanism of tRNA denaturation will await further analysis. However, one feature is worthy of note. The CCA stem projects out and appears free from contacts with the rest of the molecule. It seems to us entirely possible that this stem may be capable of changing

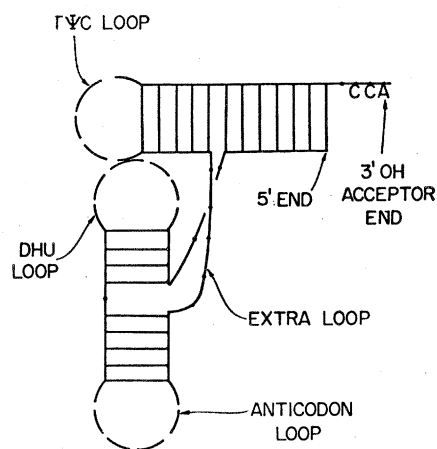


Fig. 5. Diagrammatic representation of the yeast phenylalanine tRNA. This shows the way in which the cloverleaf representation must be transformed in order to show the physical connections between various parts of the molecule. The orientation of the anticodon loop is the same in this diagram as it is in the conventional cloverleaf representation.

its orientation somewhat either in this molecule or in other tRNA molecules. If an effect of this type does occur it could be of considerable importance in understanding various mechanisms that exist in charging tRNA. This might also be of importance during protein synthesis in the ribosome.

S. H. KIM\*, G. J. QUIGLEY  
F. L. SUDDATH, A. MCPHERSON  
D. SNEDEN, J. J. KIM  
J. WEINZIERL, ALEXANDER RICH  
*Department of Biology,  
Massachusetts Institute of Technology,  
Cambridge, 02139*

#### References and Notes

1. R. W. Holley, J. Apgar, G. A. Everett, J. T. Madison, M. Marguise, S. H. Merrill, J. R. Penwick, A. Zamir, *Science* **147**, 1462 (1965).
2. S. H. Kim, G. Quigley, F. L. Suddath, A. Rich, *Proc. Nat. Acad. Sci. U.S.A.* **68**, 841 (1971).
3. U. L. RajBhandary and S. H. Chang, *J. Biol. Chem.* **243**, 598 (1968).
4. S. H. Kim, G. J. Quigley, F. L. Suddath, A. McPherson, D. Sneden, J. J. Kim, J. Weinzierl, P. Blattman, A. Rich, *Proc. Nat. Acad. Sci. U.S.A.* **69**, 3746 (1972).
5. Abbreviations: C, cytidine; A, adenosine; Ψ, pseudouridine; T, ribothymidine; U, uridine; DHU, dihydrouridine; tRNA<sup>Val</sup><sub>1</sub>, valine tRNA, species 1.
6. Y. P. Wong, D. R. Kearns, B. R. Reid, R. G. Shulman, *J. Mol. Biol.*, in press.
7. F. Cramer, *Progr. Nucleic Acid Res. Mol. Biol.* **11**, 391 (1971).
8. M. Yaniv, A. Favre, B. G. Barrell, *Nature* **223**, 1331 (1969).
9. D. Hirsh, *ibid.* **228**, 57 (1970).
10. Supported by grants from NIH (CA 04186-15 at M.I.T. and GM 15000-04 at the Biochemistry Department, Duke University), NSF, NASA, the American Cancer Society; and by an NIH postdoctoral fellowship to G.J.Q.; American Cancer Society postdoctoral fellowships to A.M. and F.L.S.; and NIH training grants to D.S. and J.W.

\* Present address, Department of Biochemistry, Duke University, Durham, N.C. 27707

19 December 1972